

Cite this: *J. Mater. Chem. A*, 2018, 6, 7042

Nonflammable superhydrophobic paper with biomimetic layered structure exhibiting boiling-water resistance and repairable properties for emulsion separation†

Gang Wen ^{ab} and ZhiGuang Guo ^{*ab}

Commercial paper as an indispensable material in our daily life is extremely easily destroyed by water and fire. And obtaining paper with the writable, non-flammable and superhydrophobic properties is still a challenging issue. Inspired from nature, biomimetic nanowires made from hydroxyapatite (HAP) can be used as raw materials to fabricate functional paper. In this study, we present a superior, fire-resistant and repairable superhydrophobic PFDS-paper@ZnO exhibiting remarkable oil absorption–combustion performance. In particular, the layered structure of the paper might be the reason of its excellent superhydrophobicity even after 20 abrasion cycles with sandpaper (400 cW). In contrast, the common paper was destroyed after 5 abrasion cycles with sandpaper under identical conditions. It was observed that the intrinsic fire-resistant nature of the paper was expected to reduce the risk of fire and might be used as an absorbent for flammable oil. On the one hand, such burnt paper can recover its original superhydrophobicity by facile modification after multiple cycles, achieving the repairable performance of its superhydrophobic surface. On the other hand, the burnt paper without subsequent modification exhibits superhydrophilicity in air and also underwater superoleophobicity, which can be used for efficient surfactant-stabilized oil-in-water emulsion separation. This study expands the potential applications of functional paper, which might be a breakthrough for traditional papermaking industries.

Received 28th February 2018
Accepted 21st March 2018

DOI: 10.1039/c8ta01920g

rsc.li/materials-a

1. Introduction

Cellulose-based paper is a green and sustainable product that has become an indispensable part of our daily life due to its wide variety of applications in the field of packing, storage and delivering information.^{1–5} Considering that a large number of hydroxyl groups on the surface of cellulose-based paper results in the reduction of strength,^{6–8} developing materials with tunable surface wettability is one such interesting research direction. If paper is made water repellent, then waterproof paper would be useful in various fields. Inspired by the nature, a variety of artificial superhydrophobic papers with combination of hierarchical micro- and nanostructure or micro- and sub-microstructure and low surface energy materials have been reported.⁹ Until now, coating nanoparticles,^{10,11} chemical grafting modification,¹² plasma treatment,¹³ chemical

modification of paper in the solution phase¹⁴ and rapid expansion of supercritical solutions technique¹⁵ have been proposed to prepare super hydrophobic paper. However, the abovementioned methods require specialized instrumentation and the process is generally complicated. Another problem is that it is hard to fulfill the super hydrophobic consistency.

Safety requirements are becoming increasingly drastic in terms of flammable hazards of paper and its fire resistance performance. Most types of paper are not able to resist fire and the consequences of fire are far more severe than the destruction of paper, which limits its applications to a large extent. In practical research, some flame retardant additives were added into cellulose, such as magnesium hydroxide,¹⁶ calcium carbonate,¹⁷ ammonium phosphate¹⁸ or silica-based¹⁹ flame retardants, impacting pyrolysis processes chemically by accelerating dehydration and carbonization. However, the thermal decomposition of cellulose still occurs during the combustion of paper and most of the combustion processes have environmental and safety hazards. The durability of paper towards fire is the main obstacle that hinders its further applications. This combined challenge has inspired us to develop effective and environmentally friendly flame retardant systems for paper.

Hydroxyapatite (Ca₁₀(OH)₂(PO₄)₆, HAP) as the main inorganic constituent of bone in vertebrates is an important biomaterial due

^aHubei Collaborative Innovation Centre for Advanced Organic Chemical Materials, Ministry of Education Key Laboratory for the Green Preparation and Application of Functional Materials, Hubei University, Wuhan 430062, People's Republic of China

^bState Key Laboratory of Solid Lubrication, Lanzhou Institute of Chemical Physics, Chinese Academy of Sciences, Lanzhou 730000, People's Republic of China. E-mail: zguo@licp.cas.cn; Fax: +86-931-8277088; Tel: +86-931-4968105

† Electronic supplementary information (ESI) available. See DOI: 10.1039/c8ta01920g

to its properties of non-toxicity and biocompatibility.^{20–22} With the advantages of being green and sustainable, HAP-based materials have been increasingly investigated by both research and industry. Zhu *et al.*²³ synthesized ultralong hydroxyapatite nanowires, which were the perfect candidate for constructing paper. The intrinsic fire-resistant nature of the raw HAP nanowires of the paper is thus expected to reduce the risk of fire and can be used as an adsorbent for flammable oils. ZnO is an attractive candidate for surface applications due to its nontoxicity, low-cost and controllable structure.^{24–27} Moreover, ZnO particles can increase the surface roughness of materials and thus, they are promising additives for fabricating superhydrophobic surfaces.

Inspired by these research findings, herein, we present a robust, fire-resistant and repairable superhydrophobic paper by synthesizing raw HAP nanowires with ZnO, followed by modification with low-surface-energy material 1H,1H,2H,2H-perfluorodecyltriethoxysilane (PFDS) *via* a facile method. Compared to traditional commercial paper, the following attributes of the PFDS-paper@ZnO are demonstrated: (1) excellent superhydrophobicity and superoleophilicity, by which the water contact angle is about 153° and sliding angle is about 5°; (2) remarkable self-cleaning and anti-fouling properties, due to which the paper is does not contaminated by dirt and wetted by common liquids; (3) admirable fire-resistance, due to which the paper does not get damaged by fire; (4) superb boiling-water resistance, due to which the paper maintains its superhydrophobic performance after immersion in boiling water; (5) favorable acid and alkali resistance; (6) outstanding mechanical property, due to which no visible difference is observed in the layered structure of paper after severe abrasion. In addition to these excellent attributes, it is noted that the obtained paper exhibits excellent adsorption performances, involving a high adsorption capacity and extraordinary recyclability, through a combination of its superhydrophobicity, superoleophilicity and three-dimensional network structure. When the oil adsorbed in the paper was completely burnt, the performance of superhydrophobicity was completely lost. Fantastically, after the paper was soaked in PFDS ethanol solution for 3 h, its superhydrophobicity recovered and subsequently, the paper was able to conduct oil adsorption, indicating the repairable property of the superhydrophobic paper. Moreover, the burnt paper without subsequent modification exhibited superhydrophilicity in air and also superoleophobicity underwater, which can be used for efficient surfactant-stabilized oil-in-water emulsion separation. From the perspective of the industry this type of paper can cause less water pollution and reduce energy consumption. This study therefore provides new inspiration for the traditional papermaking industry and highlights the potential and diverse applications of inorganic paper.

2. Experiment

2.1 Materials and chemicals

Calcium chloride (CaCl₂), sodium dihydrogen phosphate (NaH₂PO₄·H₂O), sodium dodecylsulphate (SDS) and zinc oxide (ZnO) were purchased from Guangzhou XILONG Chemical Reagent Co. Ltd, China. Sodium hydroxide (NaOH) and oleic

acid were purchased from Tianjin LIANLONGBOHUA Chemical Reagent Co. Ltd, China. Carboxymethyl cellulose (CMC) was purchased from Meryer Chemical Technology Co. Ltd, China. 1H,1H,2H,2H-Perfluorodecyltriethoxysilane (PFDS) was purchased from TCI. Co. Ltd, Japan. All chemicals were used as received.

2.2 Preparation of HAP nanowires

HAP nanowires were synthesized based on a previous study.²³ Briefly, CaCl₂ (0.22 g) aqueous solution (20 mL), NaOH (1.00 g) aqueous solution (20 mL), and NaH₂PO₄·H₂O (0.28 g) aqueous solution (10 mL) were added drop-wise into the mixture containing ethanol (12.00 g) and oleic acid (12.00 g) under magnetic stirring. Then, the mixture was transferred into a 100 mL Teflon-lined steel autoclave. The autoclave was kept at 180 °C for 24 h under standard conditions. After cooling, the HAP nanowires were stirred in ethanol and water for 12 h, in sequence. Subsequently, the solution was centrifuged and stored in ethanol for the subsequent experiments. The well-dispersed HAP nanowires appeared like a wood-like suspension (Fig. S1†).

2.3 Preparation of paper@ZnO

To enhance the strength of the paper, 1 g CMC was dissolved in 120 mL water, forming a viscous solution. Then, 3 mL CMC aqueous solution was added into the ethanol containing HAP nanowires. On the one hand, after filtration through a vacuum pump, followed by drying at 60 °C, the raw paper was obtained. On the other hand, ZnO (powder, 0.1 g) aqueous solution (100 mL) and 1 mL NH₃·H₂O were added into the above solution. Under continuous and vigorous stirring for 12 h, the mixture was filtered using a vacuum pump and dried at 60 °C to obtain white and uniform paper.

2.4 Surface modification for superhydrophobic paper

In order to achieve superhydrophobicity of paper, the white paper was soaked in 100 mL 0.3% PFDS ethanol solution for 3 h. Then, the super hydrophobic paper was dried at 60 °C. Finally, the white and smooth superhydrophobic paper was obtained.

2.5 Emulsion separation

In order to obtain stable oil-in-water emulsion, 0.01 g SDS was added to a mixture that contained 100 mL water and 1 mL oil (*n*-hexane, petroleum ether, and *n*-octane). Under continuous and vigorous stirring for 6 h, the surfactant-stabilized oil-in-water emulsion was prepared. Next, the burnt superhydrophilic paper was fixed in the filtration system to separate the above mentioned oil-in-water emulsion under 0.18 bar (Fig. S8†). Following this, the filtrate was collected. The flux was calculated by the volume of filtrate per unit time according to the equation: flux = V/St , where V is the volume of filtrate, S is the area of the paper for emulsion separation, and t is the testing time (5 min).

2.6 Characterization

The crystal structure was characterized by X-ray diffraction (XRD) using an X'PERT PRO diffractometer with Cu K α

radiation of 1.5418 Å wavelength at 2θ ranging from 5° to 120° . Field emission scanning electron microscope (FESEM) images were obtained on JSM-6701F with Au-sputtered specimens. The element distribution maps of the samples were obtained by energy dispersive spectroscopy (EDS, KeveX). Fourier transform infrared spectroscopy (FTIR, Thermo Scientific Nicolet iS10) was performed on the samples as KBr disks on a Bruker 1600 FTIR spectrometer. The N_2 isotherm was measured with an automatic volumetric adsorption apparatus (Micrometrics ASAP 1010) at 77 K. Three-dimensional surface imaging of the paper was carried out using Surface Imaging System atomic force microscopy (AFM, CSPM 5500). The water contact angles (WCAs) and oil contact angles (OCAs) were measured with a DSA 100 contact angle meter (Kruss Company, Germany) or JC2000D with 5 μL distilled water droplet at ambient temperature. The average WCA values were obtained by measuring the same sample from five different sites. X-ray photoelectron spectroscopy (XPS, Thermo Scientific ESCALAB 250Xi) measurement was carried out using the Al $K\alpha$ line as the excitation source. Thermogravimetric analyses (TGA) was performed on a NETZSCH STA 449C instrument using a dynamic heating rate of $10^\circ\text{C min}^{-1}$ under an atmosphere of air. Organic content in the collected water sample was calculated by the measurement of chemical oxygen demand (COD, HACH DRB 200). The size and size distribution of the emulsions were measured by dynamic light scattering (DLS) performed on a Zetasizer Nano ZS (Malvern 3600, UK). Optical microscope images of the as-prepared emulsions and the filtrates after separation were obtained *via* using OLYMPUSBX51 microscope. All photographs were taken using a Sony camera (DSCHX200).

3. Results and discussion

3.1 Fabrication and characterization of PFDS-paper@ZnO

The entire procedure is shown in Fig. 1. In order to enhance the strength, CMC was added into the HAP nanowires-based

solution, while the as-prepared paper scattered easily without CMC. The obtained paper was flexible and could be rolled up or folded easily (Fig. S2 and Movie S1†). Moreover, we experimentally found that the superhydrophobicity of raw paper cannot be directly introduced by low surface energy PFDS. As previously reported,^{28–30} it was feasible to introduce the particles for fabricating nanowires-based superhydrophobic materials. Therefore, we designed a method to achieve dual-scale roughness by using ZnO particles. Typically, the size distribution of pure ZnO by volume ranges from 400 to 900 nm, which results from the self-aggregation of ZnO nanoparticles^{31,32} (Fig. S3†). Meaningfully, introducing ZnO particles made it possible for constructing a second scale of roughness, while an inherent scale of roughness was already present due to the interlaced HAP nanowires and the PFDS functionalization, both of which are indispensable to obtain a superhydrophobic surface. In order to check the aforementioned observation, the roughness of the paper was measured. The three-dimensional AFM images are shown in Fig. S4.† The average surface roughness (R_a) values of raw paper and PFDS-paper@ZnO were 102 nm and 136 nm, respectively, demonstrating that the addition of ZnO increases the surface roughness to a large extent. Finally, superhydrophobic paper was generated by combining the rough paper with fluorinated silane. The detail mechanisms are as follows. Zinc ammine complexes were prepared using the above-mentioned process (eqn (S1)†).³³ The coordination effect between the complexes and the hydroxide of the paper resulted in a strong bonding with the paper, which contributed to the deposition of ZnO particles on the surface of the HAP nanowires (eqn (S2)†). Finally, the hydrolysis of PFDS on the surface of ZnO resulted in superhydrophobicity.³⁴ The as-prepared superhydrophobic paper is relatively thick (about 480 μm) and its weight is about 0.4 g (Fig. S5†).

As shown in Fig. 2, the SEM images of raw paper, paper@ZnO, and PFDS-paper@ZnO are presented. It can be observed that the surface of raw paper is relatively smooth and thin HAP nanowires

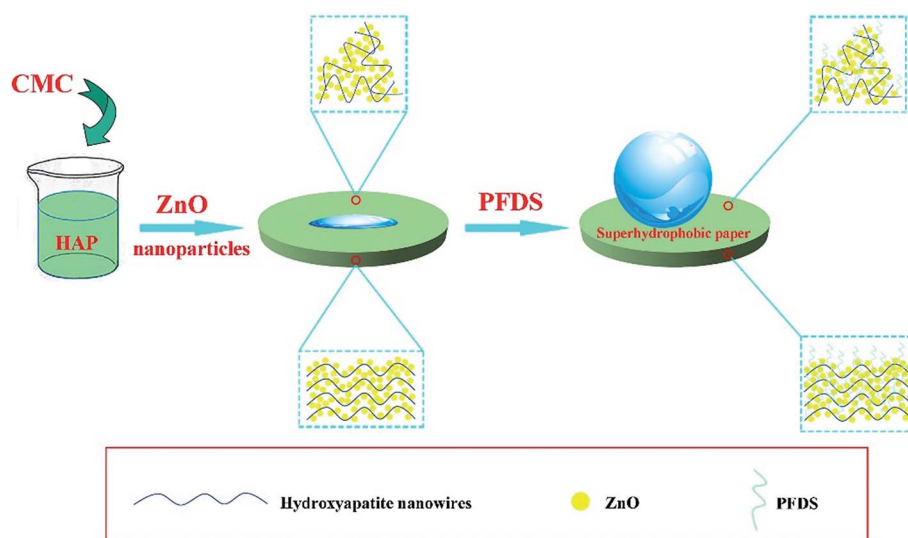


Fig. 1 Schematic illustration of the synthesis procedure of superhydrophobic PFDS-paper@ZnO from HAP nanowires.

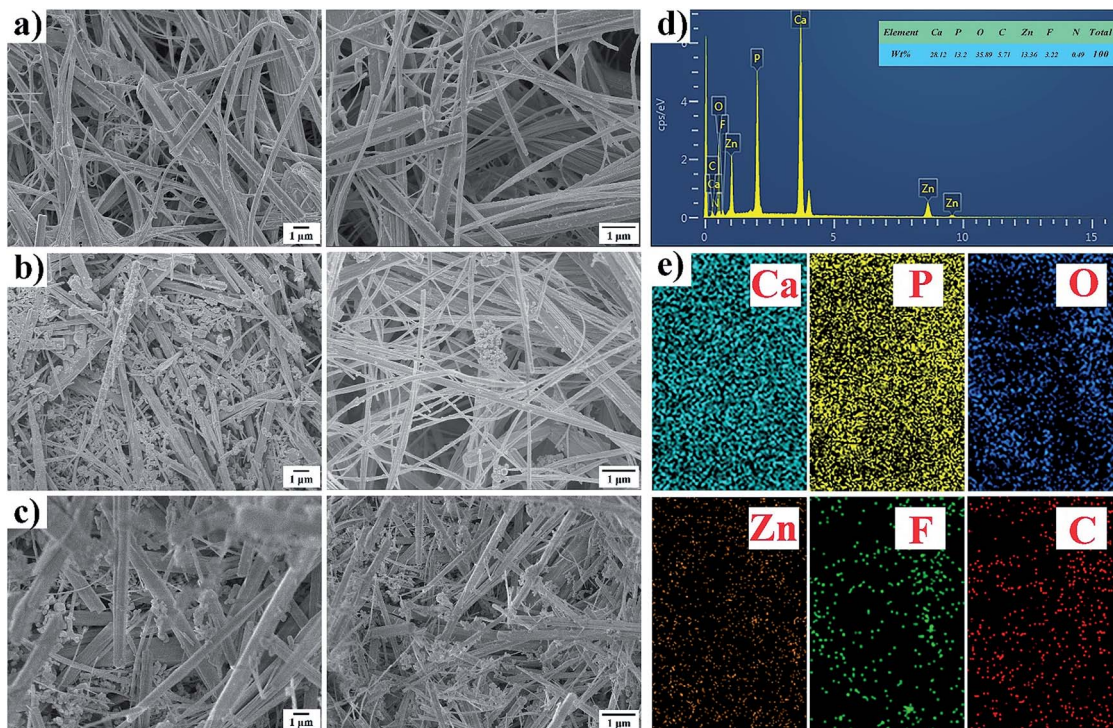


Fig. 2 SEM images of (a) raw paper, (b) paper@ZnO, (c) PFDS-paper@ZnO. (d) EDS spectra of the PFDS-paper@ZnO. (e) FESEM-EDS mapping of the PFDS-paper@ZnO.

are intertwined together like a spider's web, yielding a three-dimensional network structure with a BJH average pore size of about 14.81 nm and a specific surface area of 3.70 m² g⁻¹ (Fig. S6†). From Fig. 2b, ZnO particles can be observed intuitively and are deposited on the surface of HAP nanowires. In particular, modifying PFDS on the paper@ZnO does not alter the structure of the paper (Fig. 2c). Therefore, these post-modifications of raw paper are required to generate a surface with dual roughness, which are a prerequisite to fabricate superhydrophobic surfaces. In addition, to further validate that the ZnO particles were successfully deposited on the surface of HAP nanowires and the modification with PFDS was successful, the XRD, EDS, XPS and FTIR results were analysed. The XRD patterns of pure ZnO, raw paper, paper@ZnO and PFDS-paper@ZnO are shown in Fig. 3a; the peaks in the XRD pattern of raw paper can be indexed to a single phase of HAP with a hexagonal structure (JCPDS no. 74-0565).³⁵ All of the diffraction peaks in the XRD pattern of PFDS-paper@ZnO except for the characteristic peaks of the raw paper can be indexed to ZnO (JCPDS no. 36-1451).³⁶ The result suggested that ZnO was successfully deposited on the HAP nanowires. The EDS results indicate that PFDS-paper@ZnO mainly contains Ca, P, Zn, F, O and C elements (Fig. 2d), while raw paper contains Ca, P, O, and C elements (Fig. S7†). The contents of elements Zn and F on the surface of PFDS-paper@ZnO are relatively on the higher side. The appearance of Zn and F were separately attributed to ZnO particles and PFDS. Moreover, the SEM-EDS elemental mapping of PFDS-paper@ZnO is shown in Fig. 2e, in which the abovementioned elements are well detected. Additionally, from the results of XPS (Fig. 3c), it can be clearly seen that the raw paper is made up of O, Ca, C, and P elements,

and no Zn and F elements are observed. However, a distinct characteristic peak of Zn element appears in the spectrum of paper@ZnO, demonstrating that ZnO was successfully deposited on the surface of raw paper. Moreover, the F element is only observed in the spectrum of PFDS-paper@ZnO due to the modification of PFDS. To obtain more information on the changes of the surface compositions, we collected the high-resolution XPS data of PFDS-paper@ZnO (Fig. 3d). It can be observed that multielement spectra of O 1s centered at 532.8, 532.45, 531.20 and 530.52 eV were fitted to Zn–O–Si, Si–O–C, Zn–OH and C=O, respectively.^{37–40} Clearly, the hydrolysis process of PFDS on the surface of ZnO confirmed the Zn–O–Si bonding between ZnO and PFDS. The FTIR spectra of raw paper, paper@ZnO and PFDS-paper@ZnO were also recorded (Fig. 3b). As shown in Fig. 3c, the bands at 3565 cm⁻¹ and 633 cm⁻¹ are attributed to hydroxyl groups.⁴¹ In addition, there exist adsorption peaks of the PO₄³⁻ group (1093, 1028, 962, 604, and 561 cm⁻¹).^{42,43} The bands at 3442 cm⁻¹ and 1635 cm⁻¹ are ascribed to the absorbed water. The adsorption peaks at 2921 cm⁻¹ and 2852 cm⁻¹ are attributed to the stretching vibrations of C–H in –CH₃ and –CH₂– groups of oleic acid.⁴⁴ In addition, it is noted that the adsorption peaks at 3351 cm⁻¹ and 478 cm⁻¹ are attributed to the existence of free OH groups on the surface of ZnO and the stretching vibration of Zn & O atoms (Fig. 3d).^{45,46}

3.2 Liquid repellence, anti-fouling, and self-cleaning properties

Water droplets on superhydrophobic surfaces assume a Cassie–Baxter wetting state and easily carry away contaminants,

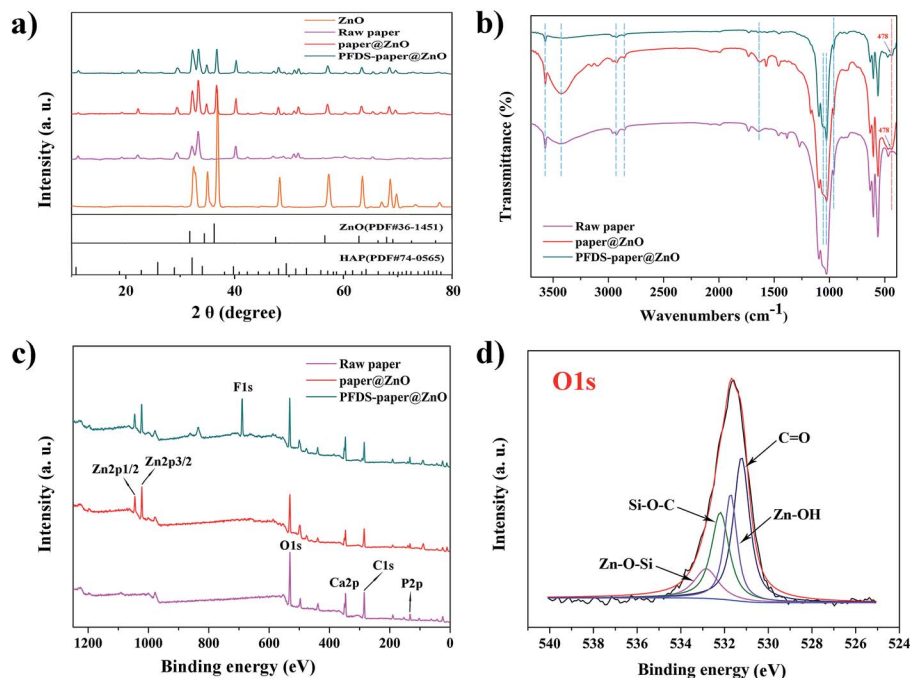


Fig. 3 (a) XRD patterns of pure ZnO, raw paper, paper@ZnO and PFDS-paper@ZnO comparing with the JCPDS database of ZnO and HAP. (b) The FTIR and (c) XPS spectra of raw paper, paper@ZnO and PFDS-paper@ZnO. (d) High-resolution O 1s XPS spectra of PFDS-paper@ZnO.

resulting in self-cleaning property. As shown in Fig. 4a–d and Movie S2–S5,[†] we poured four different drinks onto the surface of paper, namely, tea (black and green), milk and coffee, to confirm that the paper was able to remain clean. The result indicated that all droplets rolled off the horizontal superhydrophobic surface easily and no residual droplets could be observed. Further, the silver sand was taken away completely from the paper surface by water droplets, demonstrating the excellent self-cleaning performance (Fig. 4f and Movie S6[†]). The interlaced HAP nanowires and ZnO were nanoporous structures, which trapped lots of air, thus preventing the dirt from penetrating into the interior space. Hence, the paper still maintained its original state when immersed into muddy water (Fig. 4e). In addition, the nanoporous structure lowered the contact area of solid–liquid interface, which decreased the adhesion of the dirt and the paper surface. A small amount of air was trapped between liquid and paper forming an air-trap in the rough surface, which reduced the contact area between liquid and paper.

3.3 Flame-retardancy, chemical durability and boiling-water resistant property

Fire, as the basis of life, is helpful for human beings. However, disaster made by fire always leads to great loss.^{47–49} In general, paper can be burned easily by fire and the process is irreversible. Countless valuable documents are destroyed in a moment due to a fire disaster.^{50,51} Consequently, it is urgent and significant to fabricate writeable, superhydrophobic and fire-resistant paper. It is noted that inorganic nanowires paper exhibited excellent fire-resistant property owing to its intrinsic

nonflammability. In order to validate thermal stability, TG of raw paper, paper@ZnO, and PFDS-paper@ZnO were conducted under air atmosphere (Fig. 5). It was noted that the thermal decomposition temperature ranged from room temperature to 900 °C. It can be observed that the starting decomposition temperature of the PFDS-paper@ZnO is about 200 °C, which is attributed to the decomposition of the CMC.⁵² When the temperature reached to about 280 °C, the decomposition of PFDS results in the reduction of its weight percentage in the paper.⁵³ Furthermore, paper@ZnO and PFDS-paper@ZnO were relatively stable when the temperature was increased to 900 °C, similar to raw paper, validating that the weight percentage of residue of PFDS-paper@ZnO was more than 94%. There can be no doubt that PFDS-paper@ZnO possesses excellent flame-retardant property.

Hence, flame-retardant property of PFDS-paper@ZnO was further tested. A common commercial paper was referred to as a control. When burning the commercial paper, the fire spread across the entire paper and the commercial paper was reduced to ashes in four seconds even after the fire was extinguished (Fig. 6a and c). On the contrary, no evident change was observed when PFDS-paper@ZnO was subject to the same experimental conditions (Fig. 6b and Movie S7[†]). The entire burning process lasted for 8 minutes, during which the paper did not ignite at all. Interestingly, the word ‘BMT’ written on the surface of the fire-resistant paper could be easily recognized, indicating that fire had no influence on the surface of the fire-resistant paper (Fig. 6d). The flame-retardancy of this paper was attributed to the inherent non-flammable property of HAP nanowires and ZnO particles, while the cellulose-based paper does not possess such properties and hence, it was easily burned. Therefore, this

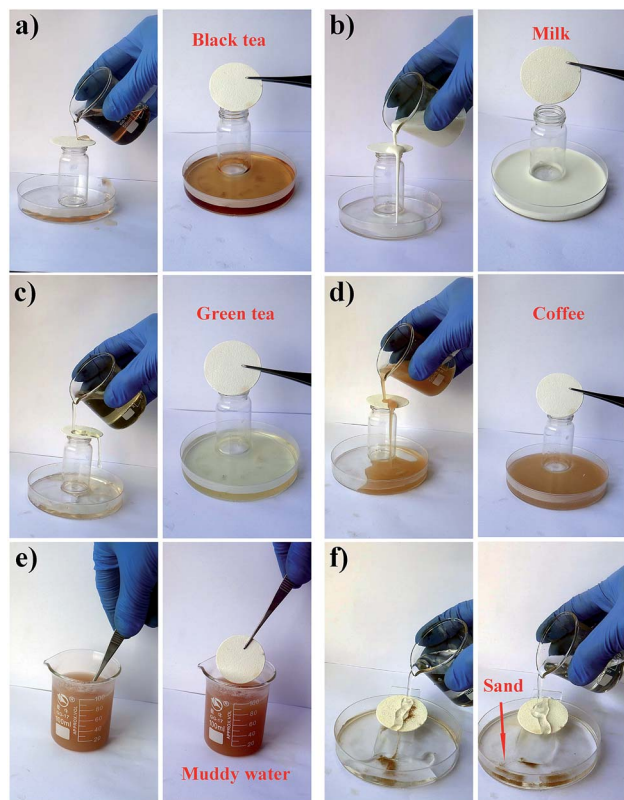


Fig. 4 Four common drinks (a) black tea, (b) milk, (c) green tea, and (d) coffee, were poured on the surface of PFDS-paper@ZnO to conduct the liquid-repellence experiment. (e) Superhydrophobic paper remains clean when immersed in the muddy water. (f) Self-cleaning experiment on PFDS-paper@ZnO with a 30° incline; silver sand as the contaminant was taken away by the water droplets.

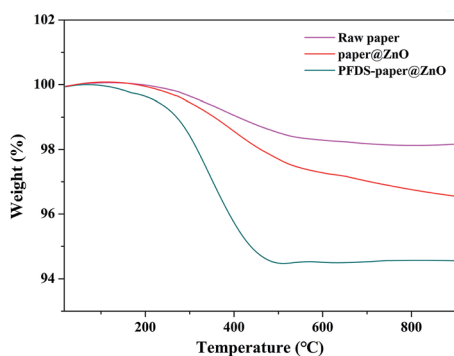


Fig. 5 TGA curves of raw paper, paper@ZnO and PFDS-paper@ZnO.

type of paper can be used for the protection of valuable documents. Furthermore, the fire-resistant property was studied and discussed later (Fig. 9).

The chemical durability of superhydrophobic paper was also evaluated by measuring its WCAs after treatment with corrosive droplets. As shown in Fig. 7a, the WCAs of the water droplets at pH = 3 and pH = 11 on the surface of super hydrophobic paper are all larger than 150°. To investigate the surface state of the superhydrophobic paper after treatment with corrosive

droplets, surface observation was performed. Fig. S8 and S9† show the EDS and SEM images of the superhydrophobic paper after treatment with corrosive droplets. The results indicate that the contents of elements Zn and F are high and no distinct change can be observed in the structure of the superhydrophobic paper. These results indicated that the superhydrophobic paper had chemical durability toward corrosive droplets.

It is well known that the superhydrophobicity of most superhydrophobic surfaces can be easily destroyed by hot water due to the decrease of surface tension of water. In order to evaluate boiling-water resistance property, the durability of the superhydrophobic paper was evaluated by monitoring its WCAs after it was immersed in boiling water. As shown in Fig. 7b, the superhydrophobic paper could tolerate boiling for 120 s with WCAs larger than 150°, while the shape of the paper was damaged. In order to confirm that the structural and chemical composition remained unchanged, EDS and SEM were conducted after boiling water treatment. Elements Zn and F are still observed intuitively and HAP nanowires and ZnO nanoparticles had almost the same morphology as that before boiling water treatment (Fig. S10†). Therefore, the superhydrophobic performance of PFDS-paper@ZnO in boiling water can be maintained for a long time as long as the paper remains integrated. These results indicated that the compact porous structure and low surface energy of the paper contributed to trapping adequate air between the boiling water and the paper, which can effectively reduce the boiling water contact area. In other words, this observation was attributed to the micro- and sub-microscale roughness and low surface energy of PFDS-paper@ZnO.

3.4 Mechanical properties

The mechanical durability of superhydrophobic surface, as one of the most important factors that limits the practical applications of paper, has an effect on the properties of materials.⁵⁴ In general, roughness of superhydrophobic surface is made up of micro- and nano-hierarchical structures, which are relatively weak and could be easily destroyed.^{55–57} Moreover, the process of destruction is irreversible despite subsequent treatment. Alternatively, the water-proof property of most common superhydrophobic surfaces is only limited to the outer surface, and the superhydrophobicity will be lost easily after abrasion. To solve these drawbacks, some research had been delivered based on the hierarchical structure.^{58–60} Herein, the PFDS-paper@ZnO is a layered structure and hence, the superhydrophobicity is exhibited by each layer. Therefore, the superhydrophobic paper retains its original property after abrasion.

In order to validate the above-mentioned mechanism, an abrasion test was conducted on the superhydrophobic paper. The paper was placed on the sandpaper (400 cW) and loaded with 200 g weight, which was dragged by steel wire for the length of 10 cm (Fig. 8a and Movie S8†). The aforementioned abrasion process was defined as one abrasion cycle. The WCAs and SAs with five abrasion cycles each are shown in Fig. 8b. With the increase in number of cycles, the WCA slightly

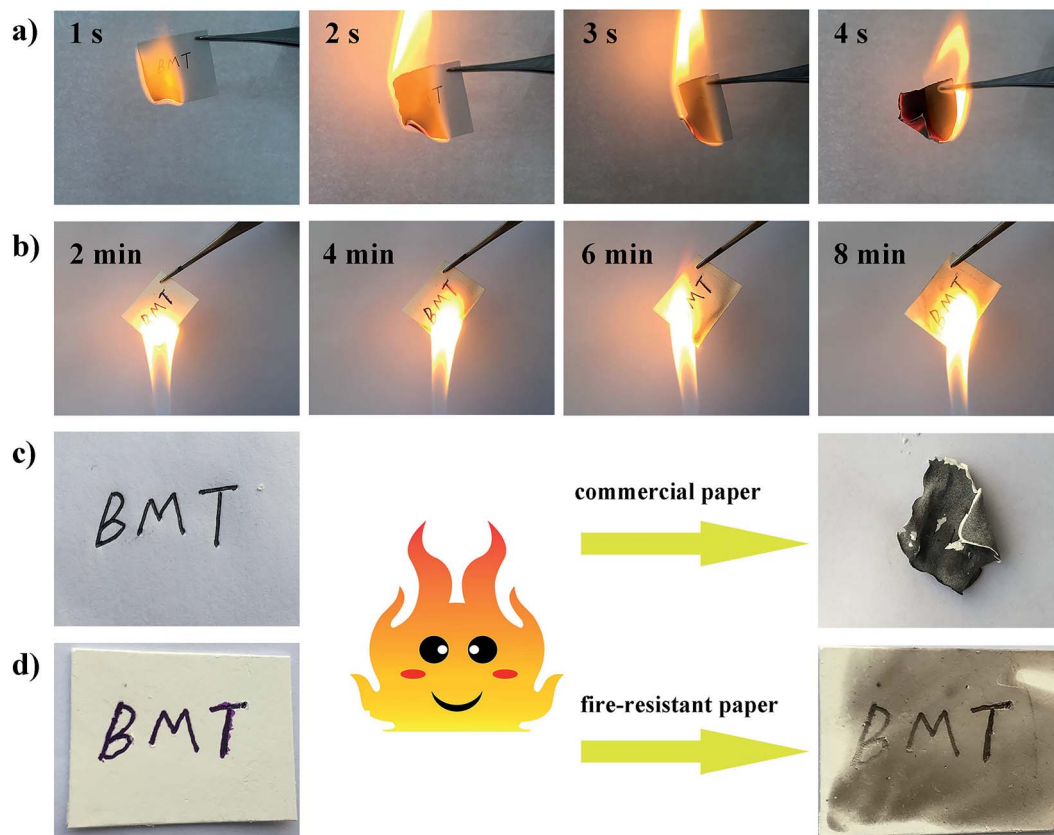


Fig. 6 Fire-resistant tests. Combustion processes and changes of (a) common commercial paper and (b) PFDS-paper@ZnO. (c) Common commercial paper is burnt into ashes. (d) No obvious change of PFDS-paper@ZnO can be observed after being burnt.

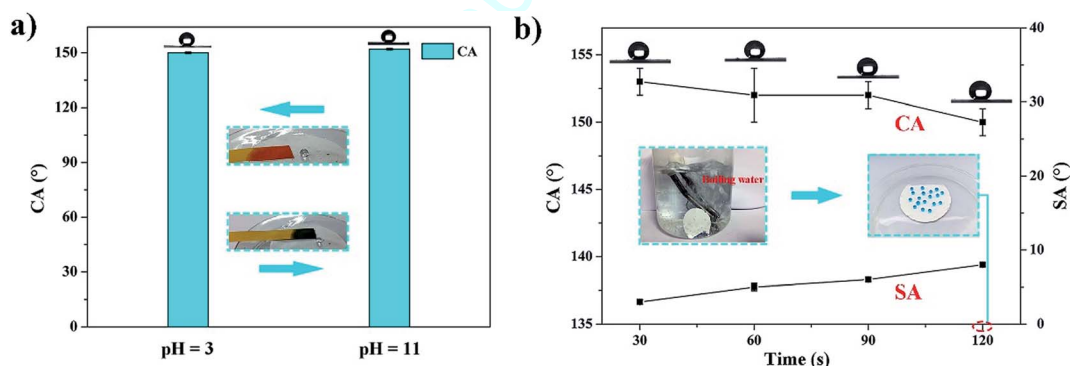


Fig. 7 (a) The WCAs of water droplets with pH = 3 and pH = 11 on the superhydrophobic paper surface. (b) The effect of boiling time on the WCAs and SAs of the PFDS-paper@ZnO in boiling water. Corresponding photographs of water droplets are shown as insets.

decreased and the SA slightly increased. However, the worn surface still exhibited superhydrophobicity when WCA was about 152° and SA was about 7° even after 20 abrasion cycles. The abrasion did not impact the wettability of the paper and the word "LICP" made by different color water droplets remained visible on the paper surface (inset of Fig. 8b). Therefore, we boldly speculate that the structure of the paper is well preserved. In order to confirm the speculation, cross-sectional view SEM was conducted after 20 abrasion cycles. Importantly, no distinct change is observed in the microscopic surface

topography after 20 abrasion cycles and the layered structure of the superhydrophobic paper remained present (Fig. 8c), confirming that abrasion treatment had no effect on the morphology of the paper. These results indicated that the as-prepared PFDS-paper@ZnO has considerable mechanical durability, which was attributed to the layered structure. Although the top view layer was destroyed, the subsequent identical structure could ensure the superhydrophobicity of the paper. Thus, the superhydrophobic paper can tolerate common physical damages.

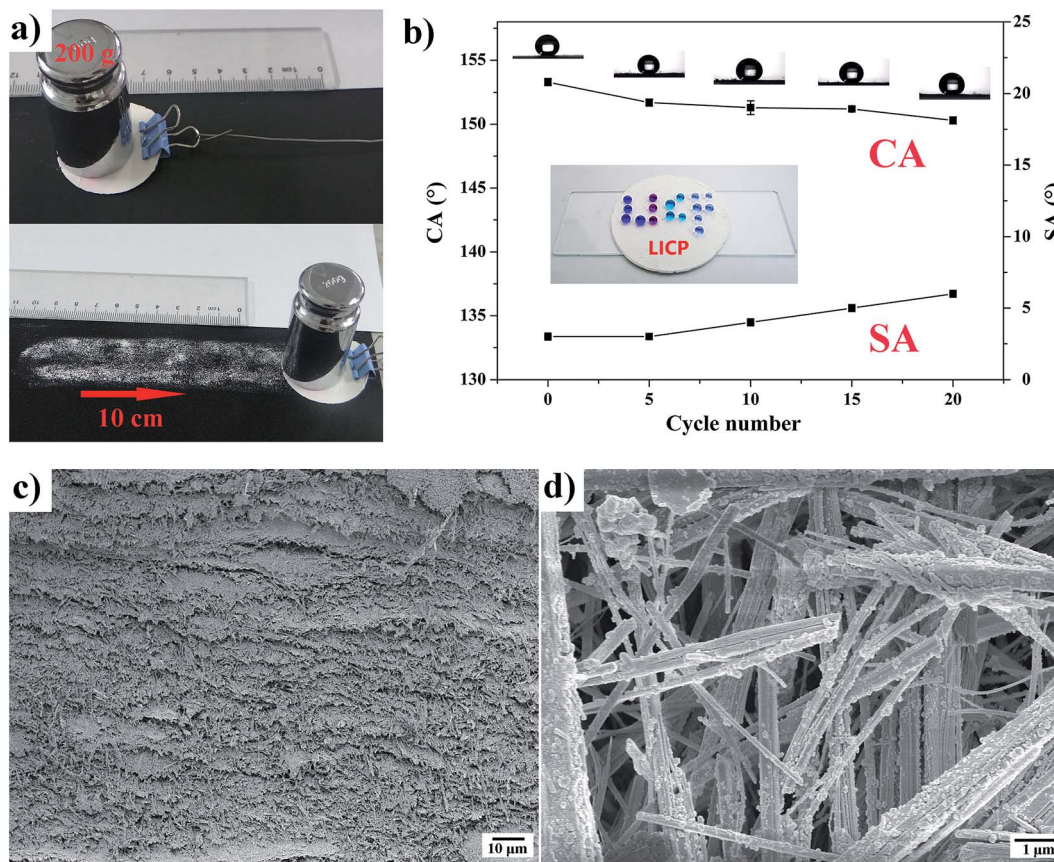


Fig. 8 Mechanical damages induced on PFDS-paper@ZnO surface. (a) Sand paper (400 cW) abrasion with 200 g load. (b) Water contact angle and sliding angle of superhydrophobic paper after each abrasion test cycle and optical image of different color water droplets on the surface of superhydrophobic paper (inset). (c) SEM image of the cross section of superhydrophobic paper after abrasion. (d) SEM image of superhydrophobic paper after abrasion test.

3.5 Oil adsorption–combustion and repairable wetting property

With the increasing industrial development, oil leakage has caused severe environmental and ecological damage.^{61,62} Aside from economic loss, the oil is generally flammable and the spilled oil usually leads to a risk of fire. Moreover, once the oil is ignited, fire disaster will occur and the situation will be extremely dangerous.⁶³ Moreover, removing even a small amount of oil from water is difficult in our daily life. Therefore, it is imperative to explore high-performance absorbable oil materials that are non-flammable.

We made full use of the performance of superhydrophobic and superoleophilic PFDS-paper@ZnO to conduct the oil adsorption–combustion experiment. To investigate the oil/water separation performance of the PFDS-paper@ZnO, *n*-hexadecane (dyed by Sudan red IV for a clear observation), regarded as an absorbable oil, was used. When the superhydrophobic paper was immersed into the layered mixture of oil and water, oil was rapidly absorbed on the paper and the color of the paper became red gradually (Fig. 9a). Clearly, hardly any oil remained in water. Simultaneously, the red paper was taken out and burned by fire. Finally, the paper became white and lost its superhydrophobicity (Fig. 9b). The oil adsorption property is

attributed to the three-dimensional interconnected network and porosity of the PFDS-paper@ZnO and the loss of superhydrophobicity resulted from the decomposition of PFDS.

What astonished us the most was that the burned paper recovered its superhydrophobic property when immersed in PFDS ethanol solution for 3 h. The oil adsorption–combustion experiment could be carried out repeatedly. The above-mentioned process was defined as one cycle. Water droplets and corresponding WCA of each of the five cycles are shown in Fig. 9d. Importantly, the paper remained intact and exhibited excellent repairable superhydrophobicity and high-performance oil adsorption ability even after 35 cycles as evidenced by the water contact angle of 151°. To confirm that the structure was not destroyed after 35 cycles, the XRD pattern and SEM image of the cycled superhydrophobic paper were recorded. The water droplet remained spherical shape on the surface of the cycled paper and no apparent difference was observed in the structure of paper after 35 cycles (Fig. 9c and S11†). The PFDS decomposed on burning the paper with flammable oil. However, HAP nanowires and ZnO particles were well-preserved, which could be modified with PFDS. Thus, the superhydrophobicity of the burned paper recovered. This fantastic discovery makes it possible for adsorbing

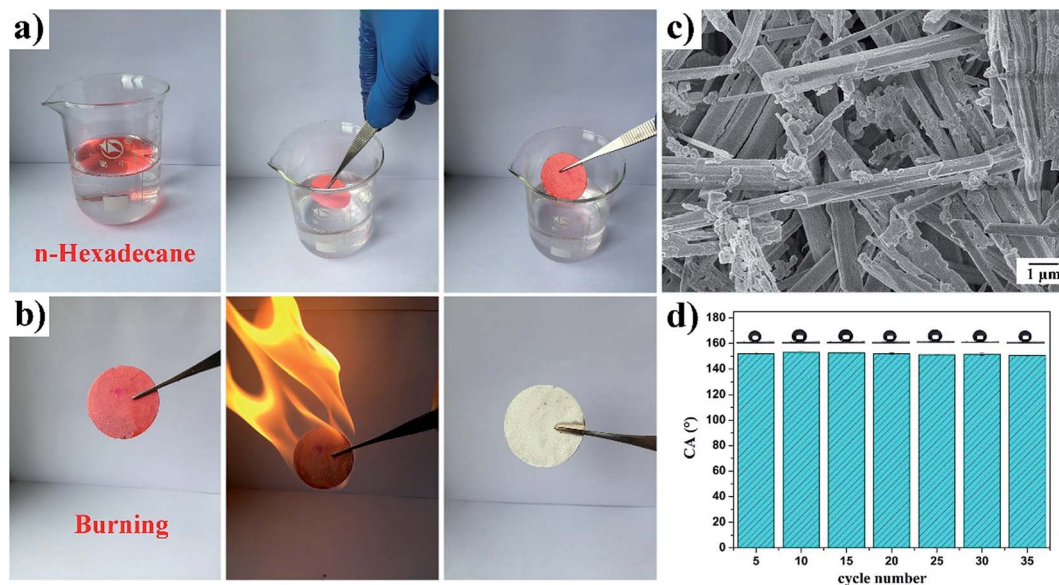


Fig. 9 Oil adsorption-combustion test. (a) Photographs showing the oil adsorption process of *n*-hexadecane by using PFDS-paper@ZnO taken at interval of 5 s (*n*-hexadecane was dyed by Sudan red IV for a clear observation). (b) Photographs showing combustion process of hexadecane-containing superhydrophobic paper. (c) SEM images of PFDS-paper@ZnO after oil adsorption-combustion test. (d) Change in CA of water droplet during repairable test. One experiment consists of 5 complete cycles when the oil-containing paper was burned and immersed in PFDS ethanol solution in repairable experiment.

a small amount of oil from water in our daily life instance, while common paper is inefficient and unrecoverable.

3.6 Separating surfactant-stabilized oil-in-water emulsion

The aforementioned experimental results demonstrated that the burnt paper recovered its superhydrophobicity when immersed into PFDS ethanol solution. Apart from this feature, additional characteristics deserve to be explored. To our

surprise, the burnt paper exhibited superhydrophilicity in air and also underwater superoleophobicity. Therefore, for the porosity and selective wettability of the burnt paper, it encourages us to further study its performance and explore oil-in-water emulsion separation. However, it was difficult to permeate the water in the emulsion through the paper under gravity in this experiment. Therefore, all experiments were conducted under 0.18 bar (Fig. S12, Movie S9†).

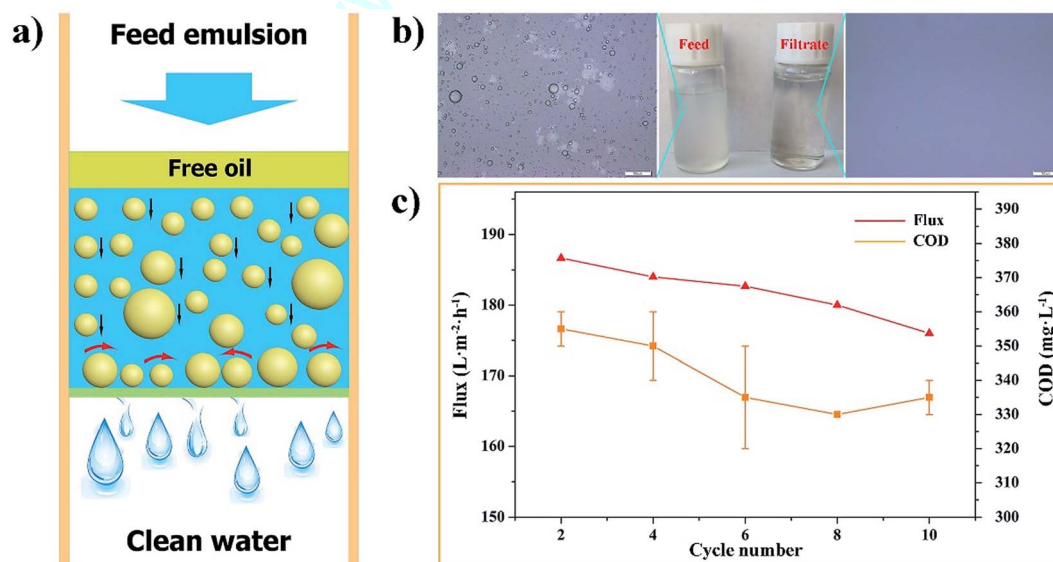


Fig. 10 (a) Schematic of separation of surfactant-stabilized oil-in-water emulsion. (b) Optical microscopy images of *n*-octane-in-water emulsion (left) and the collected filtrate (right). (c) Flux of *n*-octane-in-water emulsion separation and COD values in the collected filtrates. One experiment consists of 2 complete cycles.

Three typical SDS-stabilized oil-in-water emulsions (*n*-hexane, petroleum ether, and *n*-octane) were prepared as the model emulsions. In most cases, surfactant-stabilized oil-in-water emulsions are more difficult to treat than free oil-in-water mixtures. The OCAs of *n*-hexane, petroleum ether, and *n*-octane are shown in Fig. S13.† The paper exhibited superoleophobic properties under water with the OCAs of 151°, 153°, and 153°. When the oil-in-water emulsion touched the burnt paper, water immediately spread and permeated into the paper owing to the affinity. Moreover, a stable water/solid interface was generated, which effectively blocked the contact between oil and paper (Fig. 10a). Moreover, for the interconnected porous network structures that run through the paper, the efficient pore size was much smaller than the size of the emulsion droplets.⁶⁴

Taking *n*-octane-in-water emulsion for example, compared with the milky white feed emulsion (left), the corresponding filtrate (right) was clean and transparent. Optical microscopy images are shown in Fig. 10b, in which the dense and spherical *n*-octane droplets could be seen for the *n*-octane-in-water emulsion. On the contrary, no visible *n*-octane droplets were observed in the collected water, demonstrating that all *n*-octane droplets were successfully separated by the burnt paper. In order to determine the separation performance, the average permeation flux and COD value of every two cycles were tested. In each cycle, the paper was treated to separate *n*-octane-in-water emulsions under 0.18 bar and then dried at 60 °C. The fluxes and COD were relatively stable as revealed in Fig. 10c. In detail, the flux was about 185 L m⁻² h⁻¹ and COD was about 335 mg L⁻¹, indicating the high separation efficiency of the burnt paper. Similarly, the paper could separate other emulsions with flux of 66 L m⁻² h⁻¹ and COD of 2200 mg L⁻¹ for *n*-hexane-in-water and flux of 160 L m⁻² h⁻¹ and COD of 1400 mg L⁻¹ for petroleum ether-in-water (Fig. S14 and S15†). Therefore, the burnt paper can be regarded as a candidate for efficient oil-in-water emulsion separation.

4. Conclusion

In summary, a superior repairable superhydrophobic paper made by inorganic HAP nanowires with excellent fire resistance, robust stability (against severe abrasion, boiling water and chemical durability), good recyclability, and high-performance in oil absorption-combustion was prepared through a facile method and a straightforward modification. In particular, the fire-resistant and superhydrophobic paper not only exhibited considerable anti-fouling and self-cleaning properties, but also possessed oil/water separation ability. The absorbed oil can be burned, while the paper retains its intact structure due to its intrinsic fire-resistant nature and excellent thermal stability. Significantly, the paper can recover its original superhydrophobicity by a straightforward modification after multiple cycles, thus achieving the reproducible performance at the superhydrophobic surface. Simultaneously, the layered structure of PFDS-paper@ZnO can provide high resistance to mechanical destruction. This type of paper can be used in preservation of valuable documents and in the removal of oil.

Moreover, the burnt paper without subsequent modification exhibits superhydrophilicity in air and also underwater superoleophobicity, which can be used for efficient surfactant-stabilized oil-in-water emulsion separation. This research will be a breakthrough for traditional papermaking industries and bring in the concept of superhydrophobic and fire-resistant paper to the daily life applications of people. Moreover, the fabrication method is easy to scale up due to the facile process and use of simple equipment.

Conflicts of interest

There are no conflicts to declare.

Acknowledgements

This study was supported by the National Nature Science Foundation of China (No. 51522510, 51675513 and 51735013). We would like to extend our thanks to Ms Ruochong Zhang and Ms Xiaoyu Gao for their kind suggestions.

Notes and references

- 1 L. Peng, Y. Meng and H. Li, *Cellulose*, 2016, **23**, 2073–2085.
- 2 A. Barhoum, P. Samyn, T. Öhlund and A. Dufresne, *Nanoscale*, 2017, **9**, 15181–15205.
- 3 Z. Wang, M. Yi, Z. Zhang, M. Guo, P. Lu, Z. Chen and S. Wang, *J. Bioresour. Bioprod.*, 2017, **2**, 89–92.
- 4 M. Agarwal, Y. Lvov and K. Varshney, *Nanotechnology*, 2006, **17**, 5319–5325.
- 5 B. Balu, V. Breedveld and D. W. Hess, *Langmuir*, 2008, **24**, 4785–4790.
- 6 J. A. F. Gamelas, A. Salvador, J. Hidalgo, P. J. Ferreira and A. Tejado, *Langmuir*, 2017, **33**, 927–935.
- 7 A. C. Glavan, R. V. Martinez, A. B. Subramaniam, H. J. Yoon, R. M. D. Nunes, H. Lange, M. Thuo and G. M. Whitesides, *Adv. Funct. Mater.*, 2014, **24**, 60–70.
- 8 S. H. Li, H. B. Xie, S. B. Zhang and X. H. Wang, *Chem. Commun.*, 2007, **46**, 4857–4859.
- 9 T. Arbatan, L. Zhang, X. Y. Fang and W. Shen, *Chem. Eng. J.*, 2012, **210**, 74–79.
- 10 N. Wang, D. Xiong, S. Pan, Y. Deng and Y. Shi, *Appl. Surf. Sci.*, 2016, **389**, 354–360.
- 11 H. Ogihara, J. Xie, J. Okagaki and T. Saji, *Langmuir*, 2012, **28**, 4605–4608.
- 12 R. Bongiovanni, S. Marchi, E. Zeno, A. Pollicino and R. R. Thomas, *Colloids Surf., A*, 2013, **418**, 52–59.
- 13 B. Balu, V. Breedveld and D. W. Hess, *Langmuir*, 2008, **24**, 4785–4790.
- 14 S. Li, S. Zhang and X. Wang, *Langmuir*, 2008, **24**, 5585–5590.
- 15 O. Werner, C. Quan, C. Turner and B. Pettersson, *Cellulose*, 2010, **17**, 187–198.
- 16 Y. Si and Z. Guo, *J. Colloid Interface Sci.*, 2016, **477**, 74–82.
- 17 V. Merk, M. Chanana, T. Keplinger, S. Gaan and I. Burgert, *Green Chem.*, 2015, **17**, 1423–1428.
- 18 M. Hagen, J. Hereid, M. A. Delichatsios, J. Zhang and D. Bakirtzis, *Fire Saf. J.*, 2009, **44**, 1053–1066.

- 19 I. Šimkovic, H. Martvoňová and D. Maníková, *J. Appl. Polym. Sci.*, 2005, **97**, 1948–1952.
- 20 M. I. Kay, R. A. Young and A. S. Posner, *Nature*, 1964, **204**, 1050–1052.
- 21 F. F. Chen, Y. J. Zhu, K. W. Wang and K. L. Zhao, *CrystEngComm*, 2011, **13**, 1858–1863.
- 22 D. O. Costa, S. J. Dixon and A. S. Rizkalla, *ACS Appl. Mater. Interfaces*, 2012, **4**, 1490–1499.
- 23 Y. G. Zhang, Y. J. Zhu, F. Chen and J. Wu, *Mater. Lett.*, 2015, **144**, 135–137.
- 24 N. C. T. Martins, C. S. R. Freire and C. P. Neto, *Colloids Surf., A*, 2013, **417**, 111–119.
- 25 G. Applerot, J. Lellouche, N. Perkas, Y. Nitzan, A. Gedanken and E. Banin, *RSC Adv.*, 2012, **2**, 2314–2321.
- 26 K. Han, Z. H. Zhao, Z. Xiang, C. Wang, J. Zhang and B. Yang, *Mater. Lett.*, 2007, **61**, 363–368.
- 27 P. Joshi, S. Chakraborti and P. Chakrabarti, *J. Nanosci. Nanotechnol.*, 2009, **9**, 6427–6433.
- 28 N. Nuraje, W. S. Khan, Y. Lei, M. Ceylan and R. Asmatulu, *J. Mater. Chem. A*, 2013, **1**, 1929–1946.
- 29 M. Ma, M. Gupta, Z. Li, L. Zhai, K. K. Gleason, R. E. Cohen, M. F. Rubner and G. C. D. Rutledge, *Adv. Mater.*, 2007, **19**, 255–259.
- 30 T. Darmanin and F. Guittard, *J. Am. Chem. Soc.*, 2011, **133**, 15627–15634.
- 31 Q. Y. Cheng, X. P. An, Y. D. Li, C. L. Huang and J. B. Zeng, *ACS Sustainable Chem. Eng.*, 2017, **5**, 11440–11450.
- 32 M. Spasova, N. Manolova, N. Markova and I. Rashkov, *Fibers Polym.*, 2017, **18**, 649–657.
- 33 H. Guo, P. Fuchs, K. Casdorff, B. Michen, M. Chanana, H. Hagedorfer, Y. E. Romanyuk and I. Burgert, *Adv. Mater. Interfaces*, 2017, **4**, 1600289–1600294.
- 34 L. Chen, Y. Si and Z. Guo, *J. Mater. Chem. A*, 2017, **5**, 6416–6423.
- 35 N. Monmaturapoj, *J. Met., Mater. Miner.*, 2008, **18**, 15–20.
- 36 S. Kattel, P. J. Ramirez, J. G. Chen, J. A. Rodriguez and P. Liu, *Science*, 2017, **355**, 1296–1299.
- 37 N. N. Rabin, J. Morshed and H. Akhter, *Int. J. Chem. React. Eng.*, 2016, **14**, 785–794.
- 38 J. Li, Z. Jing, F. Zha, Y. Yang, Q. Wang and Z. Lei, *ACS Appl. Mater. Interfaces*, 2014, **6**, 8868–8877.
- 39 C. X. Xu, X. W. Sun and B. J. Chen, *Appl. Phys. Lett.*, 2004, **84**, 1540–1542.
- 40 F. Yuan, S. L. Huang and J. L. Li, *J. Mater. Chem.*, 2003, **13**, 634–637.
- 41 A. Ultee, M. H. J. Bennik and R. Moezelaar, *Appl. Environ. Microbiol.*, 2002, **68**, 1561–1568.
- 42 G. Penel, G. Leroy and C. Rey, *Calcif. Tissue Int.*, 1998, **63**, 475–481.
- 43 E. P. Paschalis, E. DiCarlo, F. Betts, P. Sherman, R. Mendelsohn and A. L. Boskey, *Calcif. Tissue Int.*, 1996, **59**, 480–487.
- 44 L. Zhang, R. He and H. C. Gu, *Appl. Surf. Sci.*, 2006, **253**, 2611–2617.
- 45 M. N. Islam, T. B. Ghosh and K. L. Chopra, *Thin Solid Films*, 1996, **280**, 20–25.
- 46 L. Vayssieres, *Adv. Mater.*, 2003, **15**, 464–466.
- 47 V. Merk, M. Chanana, T. Keplinger, S. Gaan and I. Burgert, *Green Chem.*, 2015, **17**, 1423–1428.
- 48 F. Laoutid, L. Bonnaud, M. Alexandre, J. Cyesta and P. Dubois, *Adv. Mater. Sci. Eng.*, 2009, **63**, 100–125.
- 49 R. N. Rothon and P. R. Hornsby, *Polym. Degrad. Stab.*, 1996, **54**, 383–385.
- 50 J. Wan, B. Gan, C. Li, J. Aldareguia, Z. Li, X. Wang and D. Wang, *J. Mater. Chem. A*, 2015, **3**, 21907–21921.
- 51 Z. C. Xiong, Z. Y. Yang, Y. J. Zhu, F. F. Chen, Y. G. Zhang and R. L. Yang, *ACS Appl. Mater. Interfaces*, 2017, **9**, 22212–22222.
- 52 S. Sitthichai, C. Pilapong and T. Thongtem, *Appl. Surf. Sci.*, 2015, **356**, 972–977.
- 53 X. Bai, C. H. Xue and S. T. Jia, *ACS Appl. Mater. Interfaces*, 2016, **8**, 28171.
- 54 N. Wang, D. Xiong, Y. Deng, Y. Shi and K. Wang, *ACS Appl. Mater. Interfaces*, 2015, **7**, 6260–6272.
- 55 Y. Lee, S. H. Park, K. B. Kim and J. K. Lee, *Adv. Mater.*, 2007, **19**, 2330–2335.
- 56 W. Jiang, M. Mao, W. Qiu, Y. M. Zhu and B. Liang, *Ind. Eng. Chem. Res.*, 2017, **56**, 907–919.
- 57 T. H. Kim, S. H. Ha and N. S. Jang, *ACS Appl. Mater. Interfaces*, 2015, **7**, 5289–5295.
- 58 K. Koch, B. Bhushan, Y. C. Jung and W. Barthlott, *Soft Matter*, 2009, **5**, 1386–1393.
- 59 B. Bhushan, Y. C. Jung and K. Koch, *Philos. Trans. R. Soc. London, Ser. A*, 2009, **367**, 1631–1672.
- 60 B. Bhushan, K. Koch and Y. C. Jung, *Ultramicroscopy*, 2009, **109**, 1029–1034.
- 61 W. Lei, D. Portehault, D. Liu and S. Qin, *Nat. Commun.*, 2014, **4**, 1777.
- 62 H. Bi, X. Xie, K. Yin, Y. Zhou, S. Wan and L. He, *Adv. Funct. Mater.*, 2012, **22**, 4421–4425.
- 63 X. Yue, J. Li, T. Zhang and M. W. Xue, *Chem. Eng. J.*, 2017, **328**, 117–123.
- 64 M. Liu, J. Li, Y. Y. Hou and Z. G. Guo, *ACS Nano*, 2017, **11**, 1113–1119.